

Spontaneous Symmetry Breakings in Z_2 Gauge Theories for Doped Quantum Dimer and Eight-Vertex Models

Ikuo Ichinose¹ and Daisuke Yoshioka²

Department of Applied Physics, Nagoya Institute of Technology, Nagoya, 466-8555 Japan

Abstract

Behavior of doped fermions in Z_2 gauge theories for the quantum dimer and eight-vertex models is studied. Fermions carry both charge and spin degrees of freedom. In the confinement phase of the Z_2 gauge theories, these internal symmetries are spontaneously broken and a superconducting or Neél state appears as the groundstate of the doped fermions. On the other hand in the deconfinement-topologically-ordered state, all symmetries are respected. From the view point of the quantum dimer and eight-vertex models, this result indicates interplay of the phase structure of the doped fermions and that of the background dimer or the eight-vertex model. At the quantum phase transitions in these systems, structure of the doped fermion's groundstate and also that of the background dimer or eight-vertex groundstate both change. Translational symmetry breaking induces a superconducting or antiferromagnetically ordered state of the doped fermions.

1 Introduction

Study of the strongly-correlated electron systems is one of the most interesting problems in the condensed matter physics. Most of the strongly-correlated electron materials like the high-temperature(T) cuprates, the heavy fermions, etc. have various phases like the superconducting state, antiferromagnetic(AF) Neél state, etc. in very close parameter regions. This fact indicates that in those materials the charge and spin degrees of freedom of electrons correlate and interplay with each other and as a result the phase transitions occur. Then it is important to understand quantum phase transitions(QPTs) which are difficult to be described by the ordinary Ginzburg-Landau theory in terms of a *single* order parameter. Theoretical studies on the QPTs are welcome[1] but at present there is no unified and transparent understanding of the QPTs which connect various phases with *different* order parameters.

¹Electric address: ikuo@nitech.ac.jp

²Electric address: daisuke@phys.kyy.nitech.ac.jp

In this paper we shall investigate the QPTs in which various order parameters interplay with each other. In particular we are interested in the quantum dimer and eight-vertex models with the doped fermions. Roughly speaking, the “background” dimer state can be regarded as f-electrons and the doped fermions are electrons in a conduction band from the view point of the heavy fermion materials. As the dimer states can be described by a Z_2 gauge theory as it is well-known[2], the fermion doped system under study is described by a Z_2 Ising gauge theory(IGT) coupled with the fermions. The doped fermion has *both the charge and spin degrees of freedom*. Then it is interesting to see if there exists an interplay between background dimer states like valence-bond crystal or liquid and the order of charge and/or spin degrees of freedom of the doped fermions.

In the elementary particle physics, it is well known that confinement of quarks induces spontaneous chiral symmetry breaking, i.e., phase transition of confinement and that of the chiral-symmetry breaking occur at the same time. Then one can expect that similar interplay of different phase transitions occurs in the present model. We shall study this interesting possibility in this paper.

The present paper is organized as follows. In Sec.2, we shall study the IGT coupled with fermions. In particular behavior of the charge and spin degrees of freedom of the fermions is investigated in strong-coupling regions. We show that in the even IGT the superconducting state is realized, whereas in the odd IGT the Néel state appears as the groundstate. On the other hand in the weak-coupling region, any symmetry breaking does not occur. In Sec.3, we apply the above result to the quantum dimer model on the square lattice. In the valence-bond crystal phase, a dimer or the Néel like state of the fermion’s spin degrees of freedom appears. In Sec.4, we consider the doped quantum eight-vertex(q8v) model. In the ordered state of the q8v model, the doped fermions are in the superconducting phase, whereas in the disordered phase low-energy excitations are weakly interacting fermions. Section 5 is devoted for conclusion.

2 Symmetry breaking in the IGT with fermions

In this section, we shall first review the IGT and study behavior of fermions coupled with IG variables[3]. We use the Hamiltonian formalism on d -dimensional hypercubic spatial lattice.

The IG variables are defined on links of the lattice (x, ℓ) where x denotes site and the direction index $\ell = 1, \dots, d$. Obviously $(x, \ell) = (x + \hat{\ell}, -\ell)$ where $\hat{\ell}$ is the unit vector of the ℓ -th direction. Quantum state of the IGT is specified by the quantum state at each link which is a linear combination of “up” and “down” states; $c_1|\uparrow\rangle + c_2|\downarrow\rangle = (c_1, c_2)$. Then the IG operator is given by $\sigma_\ell^3(x)$, where $\sigma_\ell^3(x)$ is the Pauli spin matrix acting on the gauge-field configuration (c_1, c_2) at (x, ℓ) . Similarly conjugate variable, i.e., the electric field operator, is given by $\sigma_\ell^1(x)$. Hamiltonian of the IGT is

composed of the electric and magnetic terms,

$$\hat{\mathcal{H}}_\sigma = \Gamma \sum_{link} \sigma^1 - \kappa \sum_{pl} \sigma^3 \sigma^3 \sigma^3 \sigma^3, \quad (1)$$

where $(link)$ and (pl) denote links and plaquettes, respectively. Γ and κ in $\hat{\mathcal{H}}_\sigma$ are parameters and they are related with the gauge coupling g as $\Gamma \propto g^2$ and $\kappa \propto 1/g^2$. The above Hamiltonian is supplemented by the physical-state condition. In the *even*(E) IGT,

$$\hat{G}_x = \prod_{link \in x} \sigma^1; \quad \hat{G}_x |phys\rangle = |phys\rangle, \quad (2)$$

where $(link \in x)$ denotes the links emanating from the site x . The phase structure of the EIGT is well known. For $d = 1$, there is no phase transition and only confinement phase exists. On the other hand for $d = 2, 3$, there is a phase transition from confinement to Higgs phase as Γ/κ decreases.

The odd(O) IGT is defined by the same Hamiltonian (1), whereas the local constraint is changed to,

$$\hat{G}_x |phys\rangle = -|phys\rangle. \quad (3)$$

It is easily verified that the above constraints (2) and (3) commute with \hat{H}_σ . The OIGT is closely related with the dimer model as we explain later on[2]. Detailed phase structure of the OIGT is not known yet.

Let us introduce fermions $\psi^\alpha(x)$ ($\alpha = 1, 2, \dots, S$) and couple them to the IG field $\sigma_\ell^3(x)$. Fermion part of the Hamiltonian is given as

$$\hat{\mathcal{H}}_\psi = -t \sum_{link, \alpha} \psi_\alpha^\dagger(x) \sigma_\ell^3(x) \psi^\alpha(x + \hat{\ell}) + \text{H.c} + M \sum_x \psi_\alpha^\dagger(x) \psi^\alpha(x), \quad (4)$$

where t is the hopping parameter and the “chemical potential” M controls the fermion density $\langle \psi^\dagger \psi \rangle$. The total Hamiltonian of the system is given by

$$\hat{\mathcal{H}}_T = \hat{\mathcal{H}}_\sigma + \hat{\mathcal{H}}_\psi. \quad (5)$$

By the fermion coupling, the physical-state condition changes to

$$\hat{G}_x \cdot e^{i\pi \sum_\alpha \psi^\dagger(x) \psi(x)} |phys\rangle = |phys\rangle, \quad \text{for EIGT} \quad (6)$$

$$\hat{G}_x \cdot e^{i\pi \sum_\alpha \psi^\dagger(x) \psi(x)} |phys\rangle = -|phys\rangle, \quad \text{for OIGT}. \quad (7)$$

Let us consider the EIGT first. Effect of the coupled fermions to the phase structure will be discussed in the following section. It is shown there that the coupling of the fermions enhances the deconfinement phase but there still exists the confinement-deconfinement phase transition. In the deconfinement phase $\kappa/\Gamma \gg 1$, fluctuation of the gauge field $\sigma_\ell^3(x)$ is small and we can simply

put $\sigma_\ell^3(x) \sim 1$ (up to irrelevant gauge transformation). The fermions move almost freely and no spontaneous symmetry breaking(SSB) of the internal symmetries occurs. On the other hand in the confinement phase $\Gamma/\kappa \gg 1$, one can expect that a SSB occurs as in the most of the gauge theories. A good example is the SSB of chiral symmetry in the quantum chromodynamics.

In order to investigate the SSB in the present gauge model, we shall derive a low-energy effective model of fermions in the confinement limit $\Gamma/\kappa \gg 1$ [4]. In the leading order of Γ , the lowest-energy states are specified as $\sigma_\ell^1(x) = -1$ for all links and the fermionic sector is highly degenerate. In order to derive an effective model for the fermionic sector, we introduce the projection operator \mathcal{P} to the subspace $|\psi\rangle_{GS}$ satisfying $\sigma_\ell^1(x)|\psi\rangle_{GS} = -|\psi\rangle_{GS}$ for all links, and we put $\mathcal{Q} = 1 - \mathcal{P}$. We start with the eigenvalue problem for the original gauge-fermion system,

$$\hat{\mathcal{H}}_T|\psi\rangle = E|\psi\rangle. \quad (8)$$

By using \mathcal{P} and \mathcal{Q} , we can derive the following equations,

$$\begin{aligned} (\mathcal{P}\hat{\mathcal{H}}_T\mathcal{P} - E\mathcal{P})|\psi\rangle &= -\mathcal{P}\hat{\mathcal{H}}_T\mathcal{Q}|\psi\rangle \\ (\mathcal{Q}\hat{\mathcal{H}}_T\mathcal{Q} - E\mathcal{Q})|\psi\rangle &= -\mathcal{Q}\hat{\mathcal{H}}_T\mathcal{P}|\psi\rangle \\ \mathcal{Q}|\psi\rangle &= (E - \mathcal{Q}\hat{\mathcal{H}}_T\mathcal{Q})^{-1}\mathcal{Q}\hat{\mathcal{H}}_T\mathcal{P}|\psi\rangle \end{aligned} \quad (9)$$

From Eqs.(9), we have an eigenvalue equation in the subspace $\mathcal{P}|\psi\rangle = |\psi\rangle_{GS}$,

$$\left[\mathcal{P}\hat{\mathcal{H}}_T\mathcal{P} + \mathcal{P}\hat{\mathcal{H}}_T\mathcal{Q}\mathcal{Q}(E - \mathcal{Q}\hat{\mathcal{H}}_T\mathcal{Q})^{-1}\mathcal{Q}\hat{\mathcal{H}}_T\mathcal{P} \right] |\psi\rangle = E\mathcal{P}|\psi\rangle. \quad (10)$$

Then an effective Hamiltonian $H_e(E)$, which acts on the subspace $|\psi\rangle_{GS}$, is given by,

$$H_e(E) = \mathcal{P}\hat{\mathcal{H}}_T\mathcal{P} + \mathcal{P}\hat{\mathcal{H}}_T\mathcal{Q}\mathcal{Q}(E - \mathcal{Q}\hat{\mathcal{H}}_T\mathcal{Q})^{-1}\mathcal{Q}\hat{\mathcal{H}}_T\mathcal{P}. \quad (11)$$

Explicit form of $H_e(E)$ is obtained in the leading order of $1/\Gamma$ as follows,

$$\begin{aligned} H_e(E) \sim & -\frac{t^2}{2\Gamma} \sum_{x,\ell} \left[\psi_\alpha^\dagger(x) \psi^\alpha(x + \hat{\ell}) \psi_\beta^\dagger(x) \psi^\beta(x + \hat{\ell}) \right] \\ & -\frac{t^2}{2\Gamma} \sum_{x,\ell} \left[\psi_\alpha^\dagger(x + \hat{\ell}) \psi^\alpha(x) \psi_\beta^\dagger(x + \hat{\ell}) \psi^\beta(x) \right] \\ & -\frac{t^2}{2\Gamma} \sum_{x,\ell} \left[\psi_\alpha^\dagger(x) \psi^\alpha(x + \hat{\ell}) \psi_\beta^\dagger(x + \hat{\ell}) \psi^\beta(x) \right] \\ & -\frac{t^2}{2\Gamma} \sum_{x,\ell} \left[\psi_\alpha^\dagger(x + \hat{\ell}) \psi^\alpha(x) \psi_\beta^\dagger(x) \psi^\beta(x + \hat{\ell}) \right] \end{aligned} \quad (12)$$

where we have used

$$\mathcal{P}\{\sigma_\ell^3(x)\}\mathcal{Q}\{\sigma_{\ell'}^3(x')\}\mathcal{P} = \delta_{\ell,\ell'}\delta_{x,x'}\mathcal{P}. \quad (13)$$

$H_e(E)$ acts on the fermion sector of $|\psi\rangle_{GS}$ and resolves its degeneracy.

Let us comment on the above low-energy effective model for the strongly coupled gauge theory. From the Hubbard model at the half filling, an antiferromagnetic(AF) Heisenberg model is derived as a result of the strong *on-site repulsion*. The above effective Hamiltonian $H_e(E)$ (12) also contains the AF magnetic interactions as we see shortly. Origin of the AF magnetic interactions is *not* the on-site repulsion but the strong *attractive gauge force*. One may expect that this attractive force may induce other SSBs besides the long-range AF order, like the superconductivity. This is the case as we see in later discussion.

The fermion fields satisfy the following canonical anticommutation relations

$$\begin{aligned}\{\psi_\alpha^\dagger(x), \psi^\beta(y)\} &= \delta_\beta^\alpha \delta_{xy} \\ \{\psi^\alpha(x), \psi^\beta(y)\} &= 0.\end{aligned}\tag{14}$$

Then it is useful to define the “spin” and “charge operators”, $Q(x)$ ’s and $P(x)$ ’s,

$$Q(x) = \frac{1}{2} \sum_\alpha [\psi_\alpha^\dagger(x), \psi^\alpha(x)] = \sum_\alpha \left(\psi_\alpha^\dagger(x) \psi^\alpha(x) - \frac{1}{2} \right)\tag{15}$$

$$Q_\beta^\alpha(x) = \frac{1}{2} [\psi_\beta^\dagger(x), \psi^\alpha(x)] - \frac{1}{2} \delta_\beta^\alpha Q(x) = \psi_\beta^\dagger(x) \psi^\alpha(x) - \frac{1}{2} \delta_\beta^\alpha - \frac{1}{2} \delta_\beta^\alpha Q(x)\tag{16}$$

$$P_{\alpha\beta}(x) = \frac{1}{2} [\psi_\alpha^\dagger(x), \psi_\beta^\dagger(x)] = \psi_\alpha^\dagger(x) \psi_\beta^\dagger(x)\tag{17}$$

$$\overline{P}_{\alpha\beta}(x) = \frac{1}{2} [\psi^\alpha(x), \psi^\beta(x)] = \psi^\alpha(x) \psi^\beta(x).\tag{18}$$

Commutation relations of $Q(x)$ ’s and $P(x)$ ’s are readily obtained from Eqs.(14),

$$[Q(x), Q(x)] = [P_{\alpha\beta}(x), P_{\alpha\beta}(x)] = [\overline{P}_{\alpha\beta}(x), \overline{P}_{\alpha\beta}(x)] = 0\tag{19}$$

$$[Q_\beta^\alpha(x), Q_\delta^\gamma(x)] = \delta_\delta^\alpha Q_\beta^\gamma(x) - \delta_\beta^\gamma Q_\delta^\alpha(x)\tag{20}$$

$$[Q(x), P_{\beta\gamma}(x)] = 2P_{\beta\gamma} = -2P_{\gamma\beta}\tag{21}$$

$$[Q(x), \overline{P}_{\beta\gamma}(x)] = -2\overline{P}_{\beta\gamma} = 2\overline{P}_{\gamma\beta}\tag{22}$$

$$[P_{\alpha\beta}(x), \overline{P}_{\gamma\delta}(x)] = \delta_\beta^\gamma Q_\alpha^\delta(x) - \delta_\alpha^\gamma Q_\beta^\delta(x) - \delta_\alpha^\delta Q_\beta^\gamma(x) - \delta_\beta^\delta Q_\alpha^\gamma(x).\tag{23}$$

In terms of $Q(x)$ ’s and $P(x)$ ’s, $H_e(E)$ can be written as follows,

$$\begin{aligned}H_e(E) &= -\frac{3t^2}{2\Gamma} V + \frac{t^2}{2\Gamma} \sum_{x,\ell} [P_{\alpha\beta}(x) \overline{P}_{\alpha\beta}(x + \hat{\ell}) + \overline{P}_{\alpha\beta}(x) P_{\alpha\beta}(x + \hat{\ell})] \\ &\quad + \frac{t^2}{2\Gamma} \sum_{x,\ell} [2Q_\beta^\alpha(x) Q_\alpha^\beta(x + \hat{\ell}) + Q(x) Q(x + \hat{\ell})],\end{aligned}\tag{24}$$

where V is the total number of sites of the lattice.

Let us consider the simplest case in which the parameter α takes two values, i.e., $\alpha = \uparrow, \downarrow$.¹ Then the states at each site are explicitly given by

$$|-1\rangle, \quad \psi_{\uparrow}^{\dagger}|-1\rangle, \quad \psi_{\downarrow}^{\dagger}|-1\rangle, \quad \psi_{\uparrow}^{\dagger}\psi_{\downarrow}^{\dagger}|-1\rangle \quad (25)$$

where $|-1\rangle$ is the empty state, $\psi^{\alpha}|-1\rangle = 0$ and $Q|-1\rangle = -|-1\rangle$.

In the EIGT, only two out of four states $|-1\rangle$ and $\psi_{\uparrow}^{\dagger}\psi_{\downarrow}^{\dagger}|-1\rangle$ are the physical state for $\sigma_{\ell}^1(x) = -1$ and by Eq.(6). Then in the Hamiltonian $H_e(E)$, the terms $Q_{\beta}^{\alpha}(x)Q_{\alpha}^{\beta}(x+\hat{\ell})$ in (24) do not contribute. The groundstate of $H_e(E)$ can be written as

$$|S\rangle = \prod_x \left[u(x)|-1\rangle_x + v(x)\psi_{\uparrow}^{\dagger}(x)\psi_{\downarrow}^{\dagger}(x)|-1\rangle_x \right], \quad (26)$$

where $u(x)$ and $v(x)$ are complex constants which satisfy $|u(x)|^2 + |v(x)|^2 = 1$. Obviously, the above state $|S\rangle$ is nothing but the superconducting state. It is straightforward to calculate the expectation value of the energy for the state (26), and the lowest-energy state is obtained as $u(x) = u$ and $v(x) = \epsilon(x)v$ where $\epsilon(x) = 1(-1)$ for the even site(the odd site). Then the energy E_S is obtained as

$$E_S = -\frac{3t^2}{2\Gamma}V + \frac{t^2}{2\Gamma} \sum_{x,\ell} [-4u^2v^2 + (-u^2 + v^2)^2]. \quad (27)$$

On the other hand the density of fermions is

$$\left\langle \sum_{\alpha} \psi_{\alpha}^{\dagger} \psi^{\alpha} \right\rangle = \langle (Q+1) \rangle = 2v^2. \quad (28)$$

Therefore at the half filling, $u^2 = v^2 = 1/2$ and $E_S = -\frac{3t^2}{4\Gamma}V$.

It is not so difficult to show that the same effective Hamiltonian (24) is derived in the OIGT at *half-filled* case. In this case, exactly one fermion resides at each site and the state $\sigma_{\ell}^1(x) = -1$ is realized for all links. In the single-particle sector of the fermions at each site $\{\psi_{\uparrow}^{\dagger}|-1\rangle, \psi_{\downarrow}^{\dagger}|-1\rangle\}$, only the last two terms in $H_e(E)$ (24) operate and the model reduces to the AF Heisenberg model. At present it is established that the Neel state with the long-range AF order is the groundstate for $d \geq 2$. Therefore the groundstate of the doped fermions in the half-filled OIGT is the AF magnet.

In the following section, we shall study the phase structure of the doped IGT by the mean-field approximation(MFA) before going into detailed investigation on the doped dimer and q8v models.

3 Phase structure of the doped IGT

In this section we shall study the effect of the doped fermions to the phase structure by the MFA. We first consider the pure EIGT. It is not so difficult to derive MF Hamiltonian $\hat{\mathcal{H}}_M$ from (1). We

¹Please do not confuse the fermion index $\alpha = \uparrow, \downarrow$ with that of the Z_2 gauge state.

formally decompose $\sigma_\ell^3(x)$ into the MF U_0 and the “fluctuation” $\delta\sigma_\ell^3(x)$ from it, $\sigma_\ell^3(x) = U_0 + \delta\sigma_\ell^3(x)$. The Hamiltonian $\hat{\mathcal{H}}_\sigma$ of the IGT is written as

$$\begin{aligned}\hat{\mathcal{H}}_\sigma &= \Gamma \sum_{link} \sigma_\ell^1(x) + \kappa \left[-U_0^4 N_P - 2(d-1)U_0^3 \sum_{link} \delta\sigma_\ell^3(x) \right] + O\left((\delta\sigma_\ell^3(x))^2\right) \\ &= \Gamma \sum_{link} \sigma_\ell^1(x) + \kappa \left[-U_0^4 N_P - 2(d-1)U_0^3 \sum_{link} \sigma_\ell^3(x) + 2(d-1)U_0^4 N_L \right] \\ &\quad + O\left((\delta\sigma_\ell^3(x))^2\right),\end{aligned}\tag{29}$$

where N_P and N_L are the number of plaquettes and links of the lattice and for the d -dimensional hypercubic lattice $N_L = \frac{2}{(d-1)}N_P$. From Eq.(29) and by neglecting the terms $O\left((\delta\sigma_\ell^3(x))^2\right)$, we obtain the MF Hamiltonian

$$\hat{\mathcal{H}}_M^G = \Gamma \sum_{link} \sigma_\ell^1(x) + \kappa \left[3U_0^4 N_P - 2(d-1)U_0^3 \sum_{link} \sigma_\ell^3(x) \right].\tag{30}$$

From Eq.(30), it is straightforward to calculate the energy of the groundstate as a function of the MF U_0 . Here we introduce the gauge coupling constant g . As we stated before $\Gamma = g^2$ and $\kappa = 1/g^2$. The effective potential, i.e, *the energy of the groundstate per link*, $V_{MF}^G(U_0)$ is obtained as

$$V_{MF}^G(U_0) = \frac{3(d-1)}{2g^2}U_0^4 - \left[\left(\frac{2(d-1)}{g^2}U_0^3 \right)^2 + g^4 \right]^{\frac{1}{2}}.\tag{31}$$

In Fig.1, we show $V_{MF}^G(U_0)$ for various values of the gauge coupling g^2 . Result obviously shows that there is a first-order phase transition and at weak coupling $\langle \sigma_\ell^3(x) \rangle \neq 0$, i.e., the phase corresponding to the Higgs phase appears[5]. At present for the 3D ($d=2$) IGT, it is known that there exists a second-order confinement-Higgs phase transition whereas in the 4D ($d=3$) IGT the transition is of first-order[6].

Effect of the doped fermions is investigated easily by the MFA. We simply put $\sigma_\ell^3(x) \rightarrow U_0$ in the Hamiltonian $\hat{\mathcal{H}}_\psi$ (4) to obtain a MF Hamiltonian $\hat{\mathcal{H}}_M^\psi$,

$$\hat{\mathcal{H}}_M^\psi = -tU_0 \sum_{link} \psi^\dagger(x)\psi(x+\hat{\ell}) + \text{H.c.} + M \sum_x \psi^\dagger(x)\psi(x).\tag{32}$$

The MF Hamiltonian can be easily diagonalized by the Fourier transformation of the field operators,

$$\hat{\mathcal{H}}_M^\psi = \int (d\vec{p}) \tilde{\psi}^\dagger(\vec{p}) \left[-2tU_0 \left(\sum_{\ell} \cos p_\ell \right) + M \right] \tilde{\psi}(\vec{p}).\tag{33}$$

The energy of the groundstate per site is given by

$$V_{MF}^\psi(U_0) = -2t|U_0| \int_0^{p_F} (d\vec{p}) \left(\sum_{\ell} \cos p_\ell \right),\tag{34}$$

where the Fermi momentum p_F is determined by the density of the fermions ρ_F , e.g., $p_F = (3\pi^2\rho_F)^{1/3}$ for $d = 3$ (and positive U_0). From (34), it is obvious that $V_{MF}^\psi(U_0) \propto -t|U_0|$ and therefore the fermion doping enhances the condensation of σ_ℓ^3 , i.e., the deconfinement-Higgs phase. This result by the MFA, i.e., the linear- U_0 dependence of $V_{MF}^\psi(U_0)$, probably over estimates the fermion effect. But we expect that the above result of the *enhancement of the deconfinement phase* is qualitatively correct as it is observed in the various gauge systems.²

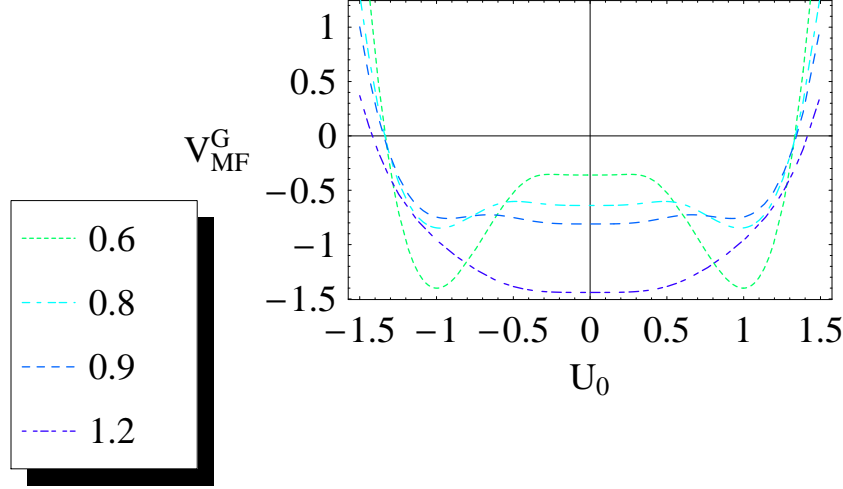


Figure 1: Effective potential $V_{MF}^G(U_0)$ of the pure EIGT with the gauge coupling $g = 0.6, \dots, 1.2$. The result indicates a first-order phase transition at $g \simeq 0.9$.

4 Doped quantum dimer model

In this section, we shall consider quantum dimer model(QDM)[8] which was introduced as a model of resonant-valence-bond (RVB) state[9]. We consider the two-dimensional square lattice for simplicity in the rest of this section. Quantum states of the model consist of closed-packed and hard-core dimers. Hamiltonian of the quantum dimer model is given as

$$H_{dimer} = \sum_{\text{plaquette}} \left[-q\mathcal{F}_P + p\mathcal{V}_P \right], \quad (35)$$

where \mathcal{F}_P is a flip term defined on each plaquette (see Fig 2.) and \mathcal{V}_P is the potential term which takes unity for flipable dimer state in the plaquette and otherwise vanishing. q and p are parameters

²Improvement of the simple MFA was discussed in various places. See for example, Ref.[7].

of the model. At the Rokhsar and Kivelson(RK) point $q = p$, the groundstate is given by the summation of all dimer configurations with equal weight; the valence-bond liquid state.

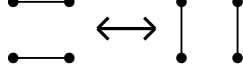


Figure 2: Flip of a pair of dimers in a plaquette. Solid lines denote dimer and dots are sites of the spatial lattice.

In the previous section we introduced the OIGT. The OIGT can be regarded as a kind of the QDM. In the OIGT description of the QDM, the state $\sigma_\ell^1(x) = -1$ on the link (x, ℓ) corresponds to the empty state, whereas that of $\sigma_\ell^1(x) = 1$ is regarded as the state occupied by a dimer. Then the physical-state condition of the *undoped* OIGT with the local constraint (3) requires that one or three dimers emanate from each site. For large positive Γ in the Hamiltonian (1), the space of states consists of closed-packed and hard-core dimers on the square lattice. On the other hand, the second term of Eq.(1) works as the flip term of two dimers that reside on a single plaquette (see Fig.2).

At present it is known that in most of the parameter region the columnar or staggered ordered state, which breaks the translational symmetry, is the groundstate of the undoped QDM H_{dimer} (35) on the square lattice[10], whereas at the RK point the translationally symmetric state is realized[2, 11, 12]. However by the doping, a liquid state of VB may appear as the groundstate in a finite parameter region[13].

In the previous section we considered the half-filled case of the doped OIGT. Here we focus on the lightly doped QDM assuming that a valence bond crystal like the columnar state is still the groundstate. Let us consider a two-fermion doped QDM first. A pair of fermions doped in the columnar state reside on the nearest-neighbor(NN) sites and a dimer on the link connecting the two sites disappears. This state is the lowest-energy state. Similarly when $2n$ fermions are doped into the QDM, there are various configurations in which n dimers disappear by the doping. Effective Hamiltonian of the doped fermions can be derived in the framework of the OIGT and the Hamiltonian of the AF Heisenberg model is obtained (up to an irrelevant constant term),

$$H_e^{dimer} = \frac{t^2}{\Gamma} \sum_{x, \ell} \left(2Q_\beta^\alpha(x)Q_\alpha^\beta(x + \hat{\ell}) + Q(x)Q(x + \hat{\ell}) \right), \quad (36)$$

where the summation is performed over the links (x, ℓ) connecting sites of doped fermions.

For an isolated pair of fermions, it is easily to obtain the wavefunction. In particular in the case $S = 2$, i.e., $\alpha = \uparrow, \downarrow$, they form a spin-singlet state,

$$\left(\psi_\uparrow^\dagger(x)\psi_\downarrow^\dagger(x + \hat{\ell}) - \psi_\downarrow^\dagger(x)\psi_\uparrow^\dagger(x + \hat{\ell}) \right) | -1 \rangle_x | -1 \rangle_{x+\hat{\ell}}, \quad (37)$$

and the energy of the spin-singlet pair is estimated from (36) as $E_{SSP} = -\frac{3t^2}{T}$. Two fermions can be put on two sites which separate more than one lattice spacing if the columnar-staggered-mixed configuration of dimers is considered (see Fig.3). However those states have higher energy compared with the spin-singlet pair state (37) regardless of their spin configurations as seen from H_e^{dimer} . In this way, we can expect that lightly fermion-doped dimer system has the groundstate with *inhomogeneous fermion density*, i.e., high and low fermion density regions appear. In the high density region, the Neél-like state for the fermion's internal degrees of freedom appears or a deconfinement-VB-liquid phase is realized. On the other hand in the low density region, a closed-packed and hard-core dimer state appears. Numerical studies are required in order to obtain detailed quantitative phase diagram of the doped dimer systems.

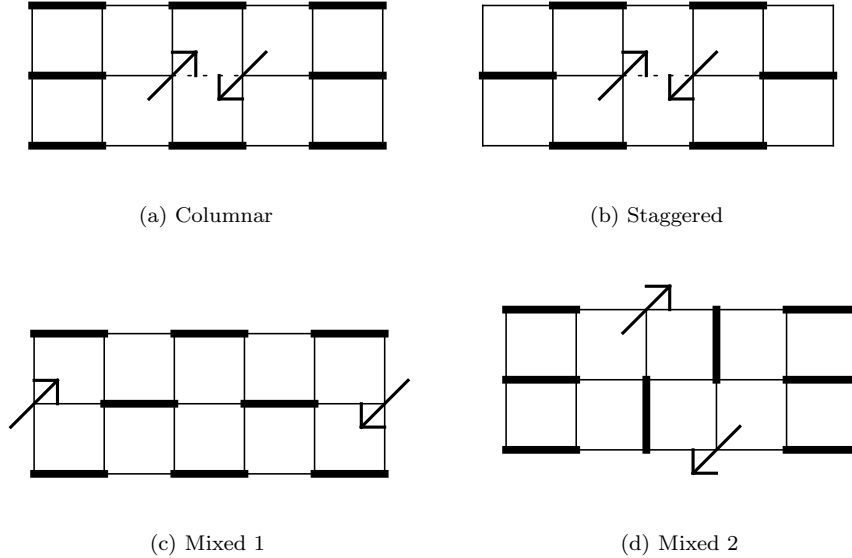


Figure 3: Configurations of fermions in dimer backgrounds: Heavy lines denote dimer. Up(down) arrow denotes spin-up(down) state of the doped fermion.

5 Doped quantum eight-vertex model as IGT

5.1 Eight-vertex model: Short review

In this section we shall investigate the behavior of doped fermions in the quantum eight-vertex(q8v) model[14]. Classical 8v model was studied by Baxter very intensively[15]. Dynamical variables are “arrows” sitting on each link of the square lattice, and then at each site four arrows meet; i.e.,

vertex. At each vertex, the numbers of incoming and outgoing arrows are both restricted to even, and therefore there are eight types of vertices, see Fig.4. For each vertex, the Boltzmann weight w_i ($i = 1, 2, \dots, 8$) is assigned and total Boltzmann weight for a configuration is simply given by the product of w_i of each vertex composing that configuration. We choose the weight w_i as follows,

$$\begin{aligned} w_1 = w_2 = a, \quad w_3 = w_4 = b, \\ w_5 = w_6 = c, \quad w_7 = w_8 = d. \end{aligned} \quad (38)$$

Hereafter, a, \dots, d also denote type of vertices. Then the partition function of classical 8v model is given as

$$Z_{c8v}(a, b, c, d) = \sum_{conf's} a^{v_a} b^{v_b} c^{v_c} d^{v_d}, \quad (39)$$

where v_a is the number of the a -type vertex in the configuration, etc.

Basis of the Hilbert space of the q8v model consists of the configuration space of the classical 8v model. Different configurations of vertices are orthogonal with each other and the norm of each configuration of vertices is normalized as unity. Hamiltonian is composed of a flip term and a potential term. The q8v model can be described by an IGT, which is the subject of the following subsection.

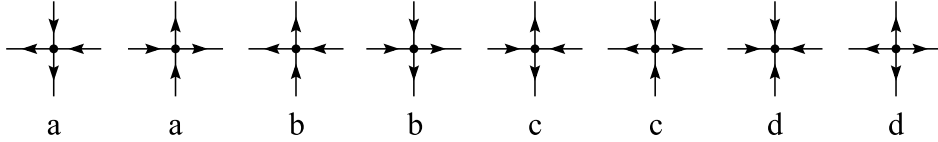


Figure 4: Vertex configurations: There are eight vertices in eight-vertex model. Their Boltzmann weight is given by a, \dots, d .

5.2 IGT for q8v model

As explained in the previous subsection, state of the q8v model is specified by assigning arrow for each link of the two-dimensional square lattice. We call the states of the up and right arrow spin-up state whereas the states of the down and left arrow spin-down state. In order to construct physical operators, let us introduce the Pauli spin matrices for each link (x, ℓ) ($\ell = 1, 2$). Let the above up-spin and down-spin states on the link (x, ℓ) be eigenstates of the operator $\sigma_\ell^1(x)$ with eigenvalue ± 1 , respectively. From the restriction on the configurations of the classical 8v model, the physical state of the q8v model must be satisfied the following local constraint,

$$\sigma_1^1(x) \sigma_1^1(x - \hat{1}) \sigma_2^1(x) \sigma_2^1(x - \hat{2}) |phys\rangle = |phys\rangle, \quad \text{for all } x. \quad (40)$$

The constraint (40) is nothing but the gauge-invariant condition in the IGT. Flip operation works on arrows on four links forming a plaquette, and then the flip term of the Hamiltonian is given as

$$H_{flip} = - \sum_{pl} \sigma_1^3(x) \sigma_1^3(x + \hat{2}) \sigma_2^3(x) \sigma_2^3(x + \hat{1}). \quad (41)$$

It is obvious that the above Hamiltonian (41) is the magnetic term of the IGT and commutes with the constraint (40).

If there are no terms in the Hamiltonian besides the flip term (41), the groundstate is the summation of all the states in the configuration space with equal weight, $a = b = c = d$. This state is nothing but Kitaev's state which may play an important role in quantum tori codes[16]. In order to give nontrivial weight for states in the q8v model, we shall introduce a potential term. To this end we consider the following operators that distinguish the verices a, \dots, d ,

$$\begin{aligned} S_a(x) &= \frac{1}{4} \left(\sigma_1^1(x) + \sigma_2^1(x) + \sigma_1^1(x - \hat{1}) + \sigma_2^1(x - \hat{2}) \right), \\ S_b(x) &= \frac{1}{4} \left(\sigma_1^1(x) - \sigma_2^1(x) + \sigma_1^1(x - \hat{1}) - \sigma_2^1(x - \hat{2}) \right), \\ S_c(x) &= \frac{1}{4} \left(\sigma_1^1(x) - \sigma_2^1(x) - \sigma_1^1(x - \hat{1}) + \sigma_2^1(x - \hat{2}) \right), \\ S_d(x) &= \frac{1}{4} \left(\sigma_1^1(x) + \sigma_2^1(x) - \sigma_1^1(x - \hat{1}) - \sigma_2^1(x - \hat{2}) \right). \end{aligned} \quad (42)$$

Operation of the above four operators is summarized in Table 1. From the Table1, it is obvious that all eight vertices are distinguished by S_a, \dots, S_d . Projection operators can be easily obtained,

$$\mathcal{P}_i = S_i^2, \quad i = a, b, c, d, \quad (43)$$

and after some calculation

$$\mathcal{P}_a + \mathcal{P}_b + \mathcal{P}_c + \mathcal{P}_d = \mathcal{I}. \quad (44)$$

Table 1: Relation between operator S_i and eight-vertex configurations

S_a	1	-1	0	0	0	0	0	0
S_b	0	0	-1	1	0	0	0	0
S_c	0	0	0	0	-1	1	0	0
S_d	0	0	0	0	0	0	-1	1

By using the projection operators \mathcal{P}_i ($i = a, b, c, d$), we can construct a potential term which assigns weight for each pure state just like the partition function of the classical 8v model (39). To

this end, let us see how vertices interchange with each other under the plaquette flip. For example the d -type vertex on left-down or right-up site(even site) of a flip plaquette changes to the a -type vertex. On the other hand, the d -type vertex on right-down or left-up site (odd site) changes to the b -type vertex. These are summarized in Table.2. We can give the potential term[14],

$$\begin{aligned}
H_V = & \sum_x \left(\frac{d}{a} \mathcal{P}_a(x) + \frac{c}{b} \mathcal{P}_b(x) + \frac{b}{c} \mathcal{P}_c(x) + \frac{a}{d} \mathcal{P}_d(x) \right) \\
& \times \left(\frac{c}{a} \mathcal{P}_a(x + \hat{1}) + \frac{d}{b} \mathcal{P}_b(x + \hat{1}) + \frac{a}{c} \mathcal{P}_c(x + \hat{1}) + \frac{b}{d} \mathcal{P}_d(x + \hat{1}) \right) \\
& \times \left(\frac{c}{a} \mathcal{P}_a(x + \hat{2}) + \frac{d}{b} \mathcal{P}_b(x + \hat{2}) + \frac{a}{c} \mathcal{P}_c(x + \hat{2}) + \frac{b}{d} \mathcal{P}_d(x + \hat{2}) \right) \\
& \times \left(\frac{d}{a} \mathcal{P}_a(x + \hat{1} + \hat{2}) + \frac{c}{b} \mathcal{P}_b(x + \hat{1} + \hat{2}) + \frac{b}{c} \mathcal{P}_c(x + \hat{1} + \hat{2}) + \frac{a}{d} \mathcal{P}_d(x + \hat{1} + \hat{2}) \right). \quad (45)
\end{aligned}$$

The total Hamiltonian of the q8v model is then given by

$$\hat{\mathcal{H}}_{q8v} = H_{flip} + H_V. \quad (46)$$

It is not so difficult to show that weight of the configuration with v_a a -type vertices etc. is given by $a^{v_a} b^{v_b} c^{v_c} d^{v_d}$ in the groundstate wavefunction $|GS(a, b, c, d)\rangle$. Then the partition function of the $q8v$ model at $T = 0$ is related with the $c8v$ model as follows,

$$Z_{q8v}(a, b, c, d) = Z_{c8v}(a^2, b^2, c^2, d^2). \quad (47)$$

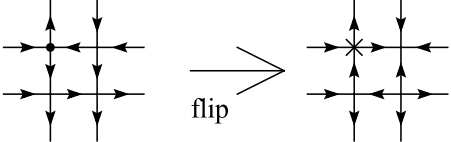
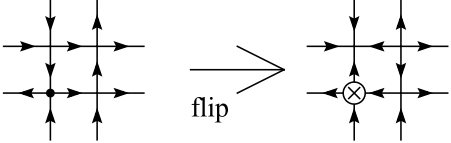
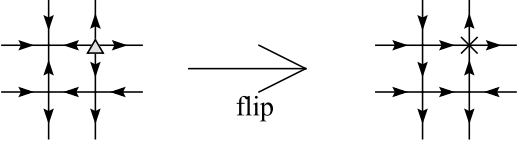
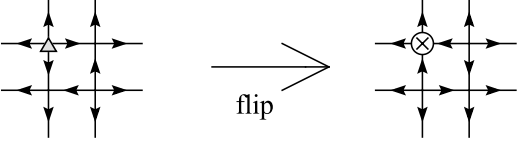
Phase structure of the classical 8v model is well-known, and from the relation (47) it gives that of the q8v model at $T = 0$. Fig.5 shows the phase diagram of the q8v model[15, 14]. We put $a = b = 1$ for simplicity. The region I (II), which is given by $c^2 > d^2 + 2$ ($d^2 > c^2 + 2$), is an ordered phase where the c -type vertices (d -type vertices) dominate. On the other hand the region III , $-2 < c^2 - d^2 < 2$ is a disordered phase and various states including all vertices appear in the wavefunction of the groundstate³. In particular at Kitaev's point $a = b = c = d = 1$, all configurations appear with the equal weight.

Let us consider fermion doping in the q8v model. In the region III (the disordered phase), doped fermions move almost freely and no SSB occurs. On the other hand in the ordered phases I and II , strong interactions work on doped fermions and we expect that some kind of SSB of the internal symmetry of fermions takes place there. This is the subject of the following subsection.

³In certain limits of the parameter space like $c^2 = d^2 \rightarrow \infty$, only c and/or d vertices appear. See later discussion.

Table 2: Relation between flip operation and eight-vertex configurations: Cross symbol and circled-cross symbol denote a -type and b -type vertices, respectively. Similarly, dot symbol is c -type, and triangle symbol is d -type vertices. Relation between types of vertices and symbols is summarized in the left table. The right table shows how vertices interchange with each other under plaquette-flip operation.

a	b	c	d
\times	\otimes	\bullet	\triangle

vertex type	before and after flipping
c	
	
d	
	

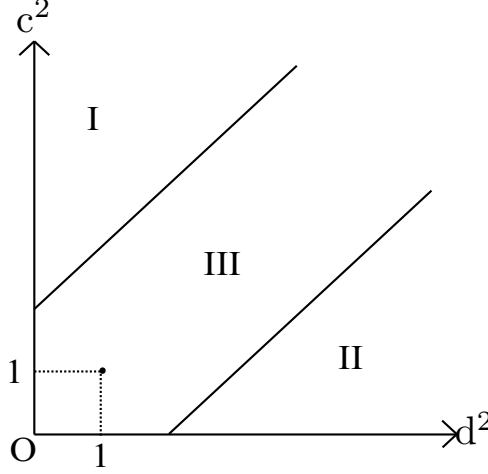


Figure 5: Phase Diagram of q8v model. Regions *I* and *II* are ordered-solid phase whereas region *III* corresponds to disordered-liquid phase. Doped fermions are in superconducting phase in region *I* and *II*. Region *III* are normal phase of doped fermions.

5.3 The limit $c^2 \rightarrow \infty$ with finite d^2

We shall consider the specific limit $c^2 \rightarrow \infty$ for investigating behavior of the doped fermions in the ordered phase. In this limit, the undoped groundstate $|GS; c\rangle = |GS(a, b, c, d)\rangle_{(c^2 \rightarrow \infty)}$ satisfies

$$\mathcal{P}_c(x)|GS; c\rangle = |GS; c\rangle, \text{ for all } x \quad (48)$$

and it is shown in Fig 6(a). Let us dope fermions in the 8v background. Fermion part of the Hamiltonian is the same with that of the IGT Eq.(4) and the total Hamiltonian of the doped q8v model is given by

$$\hat{\mathcal{H}} = \hat{\mathcal{H}}_{q8v} + \hat{\mathcal{H}}_{\psi}. \quad (49)$$

The constraint on the state (40) changes to

$$\sigma_1^1(x)\sigma_1^1(x - \hat{1})\sigma_2^1(x)\sigma_2^1(x - \hat{2}) \cdot e^{i\pi \sum \psi^\dagger(x)\psi(x)}|phys\rangle = |phys\rangle. \quad (50)$$

In the ordered phase, the gauge variables $\sigma_\ell^1(x)$'s take a definite value at each link. This means that the variables $\sigma_\ell^3(x)$ fluctuate very strongly, i.e., the *ordered phase* of the q8v model is nothing but the *confinement phase* of the IGT. This fact is pictorially observed for the limit $c^2 \rightarrow \infty$. In this case, the *undoped* system is full of *c*-type vertices (see Fig 6(a).). Then let us dope two fermions into the state $|GS; c\rangle$. In the lowest-energy state (i.e., the highest-weight state), the two fermions reside on the same site if their internal quantum number α are different whereas the fermions of the

same quantum number reside the nearest-neighbour (NN) site. In the former case, the gauge-field configuration is the same with the undoped state $|GS; c\rangle$. On the other hand in the latter case, new types of vertex appear at the sites occupied with the fermions as dictated by the local constraint (50). Then energy of the resultant gauge configuration is higher than that of $|GS; c\rangle$ by an amount c^4 , which is directly calculated from H_V . When one of fermions in a pair hops from its original position to a site with a distance L (on the lattice), L vertices change from the c -type vertices to the other ones because the hopping term of the fermion is accompanying the gauge operator $\sigma_\ell^3(x)$ which flips the arrow on the link (x, ℓ) . Then a separated pair of fermions cost energy $\sim Lc^4$. This means nothing but the confinement of the doped fermions. See Fig.6.

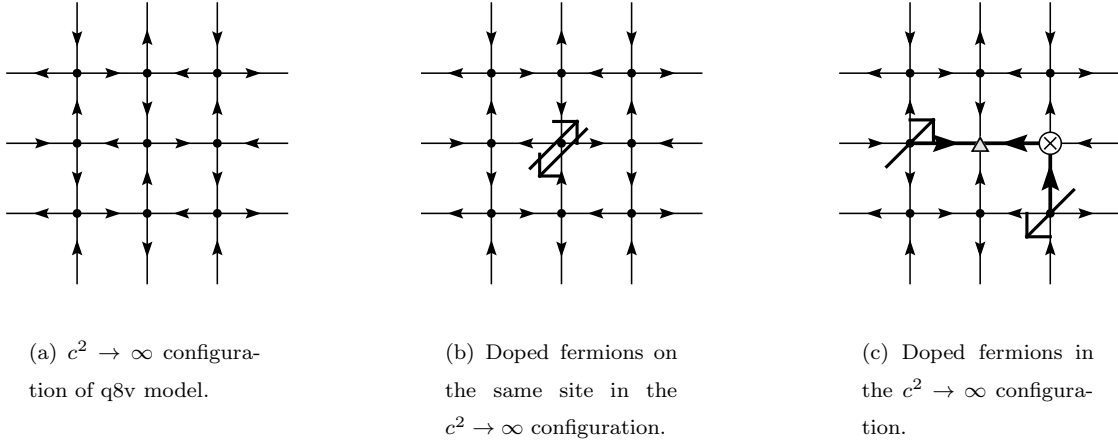


Figure 6: $c^2 \rightarrow \infty$ configurations.

Effective Hamiltonian of fermionic degrees of freedom in the ordered phase can be derived as in the previous discussion on the strongly-coupled IGT. For states with pairs of fermions residing the same sites like Eq.(26),

$$H_e^{q8v}(E) \sim \mathcal{P}_c \hat{\mathcal{H}} \mathcal{P}_c + \mathcal{P}_c \hat{\mathcal{H}} \mathcal{Q}_c \mathcal{Q}_c (E - \mathcal{Q}_c \hat{\mathcal{H}} \mathcal{Q}_c)^{-1} \mathcal{Q}_c \hat{\mathcal{H}} \mathcal{P}_c, \quad (51)$$

where $(\hat{\mathcal{H}}_{q8v} + \hat{\mathcal{H}}_\psi)|\psi\rangle = E|\psi\rangle$, $\mathcal{P}_c = \prod_x \mathcal{P}_c(x)$ and $\mathcal{Q}_c = 1 - \mathcal{P}_c$. In the leading order of c^2 ,

$$\begin{aligned} H_e^{q8v}(E) &= -\frac{16}{c^4} \mathcal{P}_c \hat{\mathcal{H}} \mathcal{Q}_c \hat{\mathcal{H}}_\psi \mathcal{P}_c, \\ &= \frac{16t^2}{c^4} \sum_{x, \ell} [P_{\alpha\beta}(x) \bar{P}_{\alpha\beta}(x + \hat{\ell}) + \bar{P}_{\alpha\beta}(x) P_{\alpha\beta}(x + \hat{\ell})]. \end{aligned} \quad (52)$$

From (52) and the discussion in Sec.2, it is obvious that the *superconducting phase* of the fermions is realized in the *ordered phase* of the doped q8v model. On the other hand in the disordered phase,

no SSBs occur. We can expect that the phase boundary of the order-disorder phase transition of the background q8v system and that of the superconductivity of the doped fermions coincide, though the region of the deconfinement phase (i.e., the disordered phase with the translational symmetry) is enlarged by the fermion doping as in the EIGT. The phenomenon that the confinement induces SSB of internal symmetry is generally observed in various gauge theories.

5.4 The limit $c^2 = d^2 \rightarrow \infty$

It is interesting and also instructive to see how the doped fermions behave in the topologically ordered phase *III*. To this end we consider the limit $c^2 = d^2 \rightarrow \infty$ with keeping $a = b = 1$. We set $c = d = K$ and take the limit $K \rightarrow \infty$. In this limit, the potential term H_V tends to

$$H_V = K^4 \sum_x (\mathcal{P}_a(x) + \mathcal{P}_b(x)) (\mathcal{P}_a(x + a_1) + \mathcal{P}_b(x + a_1)) \\ \times (\mathcal{P}_a(x + a_2) + \mathcal{P}_b(x + a_2)) (\mathcal{P}_a(x + a_1 + a_2) + \mathcal{P}_b(x + a_1 + a_2)). \quad (53)$$

From (53), the states of the lowest (vanishing) eigenvalue of H_V , $|GS; cd\rangle$, are specified by the projection operator $\mathcal{P}_{cd}(x)$,

$$\mathcal{P}_{cd}(x) = \mathcal{P}_c(x) + \mathcal{P}_d(x), \quad (54)$$

$$\mathcal{P}_{cd}(x)|GS; cd\rangle = |GS; cd\rangle, \text{ for all } x. \quad (55)$$

There are various states, besides $|GS; c\rangle$ and $|GS; d\rangle$, which satisfy the condition (55). As the flip operator H_{flip} in (41) is applied on the $|GS; cd\rangle$, the a and/or b vertices appear. Therefore in the limit $K \rightarrow \infty$, all various states in $|GS; cd\rangle$ are independent and degenerate. Among them, some symmetric configurations are depicted in Fig.7(a) and 7(b), i.e., the *c-d columnar* and *c-d staggered* configurations, respectively.

Let us dope two fermions at site x in one of the various states and move one of the fermions from x to site y . The background 8v states change from the original configuration by the fermion hopping. For the various state in $|GS; cd\rangle$, one can verify that movement of doped fermions is restricted to straight lines, i.e., the horizontal and vertical lines. Otherwise a and/or b vertices appear as a result of fermion hopping (see Fig.8). In this sense, fermions are deconfined only in one direction. In the present limit, the fermion system essentially reduces to the one-dimensional one, and therefore no SSBs take place as dictated by the Coleman theorem. This limit is in sharp contrast with Kitaev's point $a = b = c = d = 1$. At Kitaev's point, there are no potential terms of the background 8v configuration and we can simply put $\sigma_\ell^3(x) = 1$ at all links. Then the doped fermions move without any interactions.

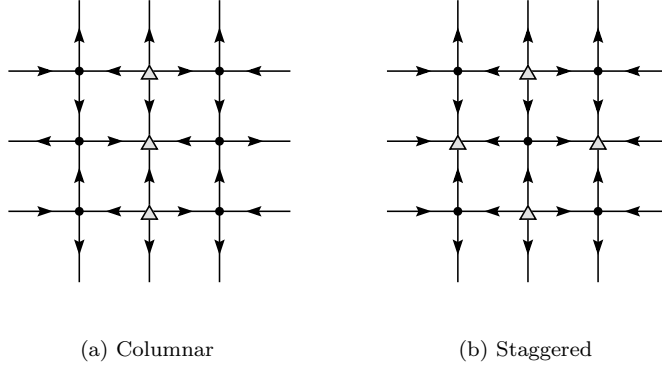


Figure 7: $c^2 = d^2 \rightarrow \infty$ configurations of q8v model.

6 Conclusion

In this paper we have studied behavior of the doped fermions in the dimer and q8v models. In most of discussion we employed the IGT description of the models. We showed that the translational symmetry breaking in the background dimer or 8v configuration induces SSBs of the internal symmetry in the doped-fermion sector. Similar phenomenon is well-known in the quantum chromodynamics in which confinement of quarks induces the SSB of the chiral symmetry of quarks. Result of the numerical studies on phase structure of the models, which shows that change of the background configuration really induces SSBs of the doped fermions, will be reported in the near future[17]. It is also very interesting to construct more realistic models similar to the models in this paper for, e.g., strongly-correlated heavy fermions and compare phase structure of the models, etc. with experiments.

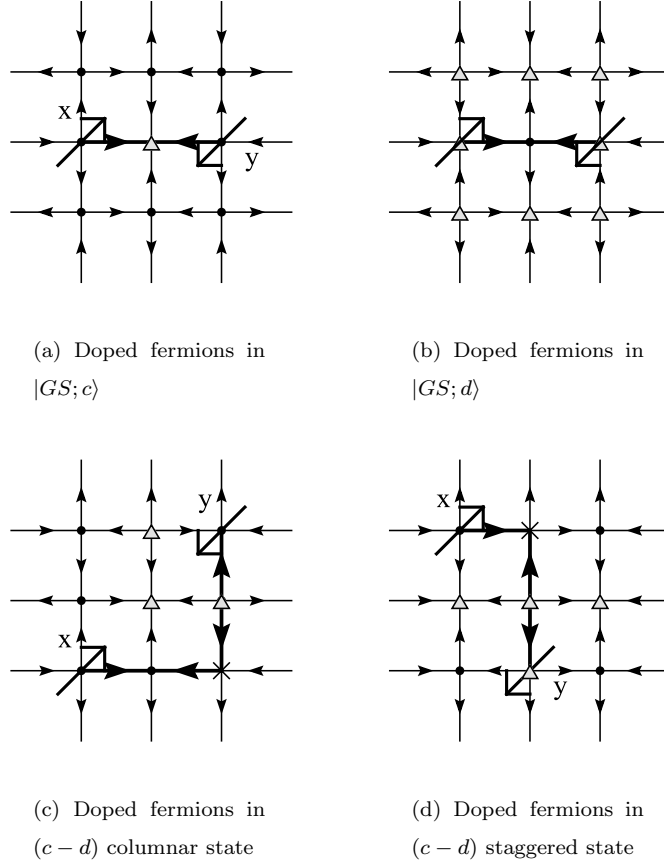


Figure 8: Fermion hopping and change of background 8v configurations. Fermion hopping in one-dimensional straightlines changes the c -vertices to the d -vertices. In the limit $c^2 = d^2 \rightarrow \infty$, resultant configurations of the 8v model have the same energy with the original ones. Therefore doped fermions move freely in the horizontal and vertical lines.

References

- [1] See for example, S.Sachdev, “*Quantum Phase Transitions*”, (Cambridge University Press, Cambridge, England, 1999).
- [2] R.Moessner, S.L.Sondhi and E.Fradkin, Phys.Rev.B65(2002)024504.
- [3] See for example, J.B.Kogut, Rev.Mod.Phys.51(1979)659.
- [4] J.Smit, Nucl.Phys.B.175(1980)307.
- [5] J.M.Drouffe, Nucl.Phys.B170(1980)211.
- [6] C.Itzykson and J.M.Drouffe, “*Statistical Field Theory*”, (Cambridge University Press, Cambridge, England, 1989).
- [7] I.Ichinose, T.Matsui and M.Onoda, Phys.Rev.B64(2001)104516.
- [8] S.A.Kivelson, D.Rokhsar and J.Sethna, Phys.Rev.B35(1987)865;
D.Rokhsar and S.A.Kivelson, Phys.Rev.Lett.61(1988)2376.
- [9] P.W.Anderson, Science 235(1987)1196.
- [10] S.Sachdev, Phys.Rev.B40(1989)5204;
L.S.Levitov, Phys.Rev.Lett.64(1990)92;
N.Read and S.Sachdev, Phys.Rev.B42(1990)4568;
P.W.Leung, K.C.Chui and K.J.Runge, Phys.Rev.B54(1996)12938.
- [11] E.Fradkin, “*Field Theories of Condensed Matter Systems*”, (Addison-Wesley, Redwood City, 1991).
- [12] R.Moessner and S.L.Sondhi, Phys.Rev.Lett.86(2001)1881.
- [13] S.Sachdev and M.Vojta, J.Phys.Soc.Jpn.69, Suppl B(2000)1.
- [14] E.Ardonne, P.Fendley and E.Fradkin, Annals of Phys.310(2004)493.
- [15] R.Baxter, “*Exactly Solved Models in Statistical Mechanics*”, (Academic Press, 1982) and references therein.
- [16] A.Yu.Kitaev, Annals Phys.303(2003)2.
- [17] D.Yoshioka and I.Ichinose, work in progress.